



# Multi-omics insights into the response of *Aspergillus parasiticus* to long-chain alkanes in relation to polyethylene modification<sup>☆</sup>

Romanos Siaperas<sup>a</sup> , George Taxeidis<sup>a</sup>, Anastasia Gioti<sup>b</sup> , Efstratios Nikolaiivits<sup>a</sup> ,  
Evangelos Topakas<sup>a,\*</sup> 

<sup>a</sup> Industrial Biotechnology & Biocatalysis Group, Biotechnology Laboratory, School of Chemical Engineering, National Technical University of Athens, Athens, Greece

<sup>b</sup> Institute of Marine Biology, Biotechnology and Aquaculture, Hellenic Centre for Marine Research, Heraklion, Greece

## ARTICLE INFO

### Keywords:

Polyethylene  
*Aspergillus*  
 Plastic modification  
 Multi-omics  
 Transcriptomics  
 Proteomics  
 Alkane assimilation

## ABSTRACT

Plastic pollution presents a global challenge, with polyethylene (PE) being among the most persistent plastics due to its durability and environmental resilience. Long-chain alkane (lcAlk) degrading microbes are a potential source of PE-degrading enzymes, as both lcAlk and PE are large hydrophobic compounds that consist exclusively of C-C and C-H bonds. In this work, we employed a multi-omics approach to study the ability of *Aspergillus parasiticus* MM36, an isolate derived from *Tenebrio molitor* intestines, to metabolize lcAlk and secrete enzymes that are potentially capable of modifying PE. The fungus was grown with hexadecane (C16) or a mixture of lcAlk (C24 to C36) as carbon sources and culture supernatants were tested daily for their ability to modify PE. Proteomic analysis identified induced oxidases hypothetically involved in lcAlk and PE functionalization. Key enzymes include multicopper oxidases, peroxidases, an unspecific peroxygenase and FAD-dependent monooxygenases. Surfactant proteins facilitating enzymatic and cellular interaction with hydrophobic substrates, such as one hydrophobin, three hydrophobic surface-binding proteins (HsbA) and one cerato platanin, were present in all secretomes. Transcriptomic analysis comparing lcAlk to C16 cultures highlighted the enrichment of oxidoreductase activities and carboxylic acid metabolism in both lcAlk incubation days, with transmembrane transporters and transferases predominating on day 2 and biosynthetic processes on day 3. In C16 cultures, hydrolytic enzymes, including esterases, were upregulated alongside Baeyer-Villiger monooxygenases, suggesting a shift toward sub-terminal hydroxylation. Integrating transcriptomic and secretomic data, we propose a mechanism for lcAlk assimilation by *A. parasiticus* MM36, involving extracellular oxyfunctionalization, hydrocarbon uptake via surface-modifying proteins and channeling through membrane transporters for energy consumption and biosynthetic processes. This study provides insights into fungal mechanisms for alkane metabolism and highlights their potential relevance to plastic biotransformation.

## 1. Introduction

Plastic pollution poses a global challenge with synthetic polymers accumulating in the environment since their mass production began in the 1950s. Fossil-based plastics are produced by polymerization of monomers derived from oil or gas and enhanced with chemical additives (Thompson et al., 2009). Among these, polyethylene (PE) stands out as one of the most prevalent plastics due to its versatility, durability and cost effectiveness accounting for over 22 % of European plastic production in 2022 (Plastics Europe, 2024). PE is a thermoplastic polyolefin, with ethylene being the single monomer unit. Its high molecular

weight, hydrophobic nature and lack of functional groups render PE exceptionally resistant, with discarded PE items persisting for decades to centuries (Chamas et al., 2020). Improper disposal and the subsequent formation of microplastics pose risks to marine life and human health through bioaccumulation (Filella et al., 2021).

Microbial degradation of plastics has emerged as a promising avenue for tackling plastic pollution. Many microorganisms, including bacteria and fungi, can assimilate carbon derived from synthetic petrochemical polymers by repurposing enzyme machinery originally evolved for degrading structurally similar natural polymers (Taxeidis et al., 2024; Zerva et al., 2021). Alkane-degrading microbes have shown potential for

<sup>☆</sup> This paper has been recommended for acceptance by Maria Cristina Fossi.

\* Corresponding author.

E-mail address: [vtopakas@chemeng.ntua.gr](mailto:vtopakas@chemeng.ntua.gr) (E. Topakas).

PE degradation. Bacteria such as *Rhodococcus* and *Alcanivorax* can grow in the presence of PE (Gravouil et al., 2017; Zampolli et al., 2021). Similarly, fungal alkane-degrading genera such as *Penicillium* and *Aspergillus* (Al-Hawash et al., 2018; Velez et al., 2020) have been reported to act on PE (Yamada-Onodera et al., 2001; Zhang, Gao, et al., 2020). Furthermore, the ability of insect larvae, particularly *Tenebrio molitor* and its gut microbiota, to degrade PE has been widely studied (Pivato et al., 2022). These larvae naturally consume beeswax, a mixture rich in alkanes, alkenes, fatty acids, and esters (Maia & Nunes, 2013). A recent study highlighted the dominance of the *Aspergillaceae* family in the gut of *T. molitor* after feeding with polypropylene, a polymer classified under polyolefins alongside PE (Wang et al., 2023).

Although PE biodegradation has been demonstrated, its underlying mechanisms remain poorly understood (Restrepo-Flórez et al., 2014). The only reported microbial PE-degrading enzymes are three laccases from *Rhodococcus* (Tao et al., 2023; Zampolli et al., 2023). Like alkane degradation, PE biodegradation is hypothesized to begin with hydroxylation either in-chain or at the termini (Jin et al., 2023). Alkane metabolism has been extensively explored at the omics level in bacteria and yeasts, but studies on filamentous fungi remain sparse. Only one transcriptomic study has examined the growth of a *Penicillium* sp. on hexadecane (C16) and hexadecene (Velez et al., 2020). For PE biodegradation, omics analyses have predominantly focused on hydrocarbonoclastic bacteria like *Rhodococcus* and *Alcanivorax* (Gravouil et al., 2017; Tao et al., 2023; Zadjelovic et al., 2022; Zampolli et al., 2021), employing transcriptomics or proteomics. Among fungi, there are only two relevant studies: a transcriptomic analysis of the marine fungus *Alternaria alternata* FB1 in the presence of PE (Gao et al., 2022), and a proteomics study on the yeast *Yarrowia lipolytica* for upcycling of depolymerized PE (Caleb et al., 2023).

Alkane chain length influences their hydrophobicity and bioavailability (Rojo, 2009). Gram-negative bacteria encode transporters able to transfer alkanes up to C38 through their outer membrane to process them intracellularly (Liu et al., 2022). Fungi can accumulate short and mid-chain alkanes like C16 (Al-Hawash et al., 2018; Li et al., 2021), but longer-chain alkanes likely require functionalization or chain scission at the extracellular space - a necessary step for PE as well (Zadjelovic et al., 2022).

Previous research demonstrated that *Aspergillus parasiticus* MM36, isolated from *T. molitor* intestines, can grow using a mixture of long-chain alkanes (lcAlk), ranging from C24 to C36, as the sole carbon source. Additionally, its lcAlk-induced secretome can interact with and induce structural modifications on low-density polyethylene (LDPE) (Taxeidis et al., 2023). To gain deeper insights into this strain's metabolic capabilities, we employed a multi-omics approach, starting with genome sequencing, assembly and annotation. We performed RNAseq to investigate the molecular response during lcAlk assimilation. Secretome analysis with LC-MS/MS provided further insights into the enzymes involved in lcAlk modification and their potential role in PE functionalization. This offers a comprehensive view of alkane metabolism by filamentous fungi and its possible implications for plastic biotransformation.

## 2. Results and discussion

### 2.1. Genomic analysis of newly isolated *Aspergillus parasiticus* MM36

*A. parasiticus* MM36, isolated from mealworm (*Tenebrio molitor*) intestines, can grow using lcAlk as the sole carbon source and its lcAlk-induced secretome causes structural modifications in PE (Taxeidis et al., 2023). To study the genetic features underlying this capability and to facilitate subsequent transcriptomic and proteomic analyses, we first performed whole genome Illumina sequencing and annotation. The assembled genome comprises 321 scaffolds totaling 39.8 Mb. Its predicted proteome includes 13844 proteins with a 99.6 % BUSCO completeness, comparable to the reference proteome of *A. parasiticus*

CBS 117618 (13752 proteins, 98.3 % completeness) (Kjærboelling et al., 2020). The repeat content in the *A. parasiticus* MM36 genome, 2.90 % as determined by RepeatMasker, is consistent with the 2–3 % average of the *Aspergillaceae* family (de Vries et al., 2017). There are 1409 transport-related genes, identified through the TCDB database (Saier Jr et al., 2021), with electrochemical potential-driven transporters, particularly the major facilitator superfamily (MFS), being the most abundant family. This family shows the highest level of expansion in the *Eurotiomyces* class (de Vries et al., 2017).

A multilocus phylogenetic analysis was conducted to confirm the species classification, as previous ITS sequence-based attempts were inconclusive. Two hundred (200) single-copy orthologs were included from 29 genomes within the *A. Flavi* section and two outgroup species. The methodology for ortholog generation and alignment was based on the work of Steenwyk et al. (2024) and the genomes were primarily sourced from the study of Kjærboelling et al. (2020). Our results confirm MM36 is part of the *A. parasiticus* species forming a well-supported clade of 100 ultrafast bootstrap and SH-like approximate likelihood ratio test with *A. parasiticus* CBS 117618 (Fig. S1). The moderate gene concordance factor (42.1 %) of this clade indicates limited signal for many single-gene trees, however 81.2 % of the informative sites also supported this clade (Minh, Hahn, et al., 2020).

### 2.2. Determining the optimal time points for multi-omics analyses

To select optimal time points for transcriptomic and proteomic analysis, we assessed the ability of *A. parasiticus* MM36 secretomes—collected from liquid cultures supplemented with C16 or lcAlk mixtures—to modify LDPE structure. Each day, the culture supernatants were collected, incubated with LDPE and the treated plastics were analysed with ATR-FTIR following the methodology detailed in a previous study (Taxeidis et al., 2023). According to ATR-FTIR spectra, the strong peaks at 2919 and 2850  $\text{cm}^{-1}$  correspond to asymmetric and symmetric  $\text{CH}_2$  stretching vibrations, respectively, while the peak at 1462  $\text{cm}^{-1}$  reflects C-H bending deformations (Gulmine et al., 2002; Kovács et al., 2021). The 1210  $\text{cm}^{-1}$  peak, associated with C-O stretching, indicates the formation of acyl groups and LDPE functionalization, while the low intensity peak at 2950  $\text{cm}^{-1}$  ( $\text{CH}_3$  stretching), observed following treatment with the isolated secretome of *A. parasiticus* MM36 after 3 days of incubation (Fig. 1), can be correlated with LDPE modification. To better interpret and compare these results, intensity ratios between the characteristic peak of LDPE at 2919  $\text{cm}^{-1}$  and newly formed peak at 1210  $\text{cm}^{-1}$  were calculated.

As presented in Table 1, the calculated ratios between the characteristic peaks at 1462  $\text{cm}^{-1}$  and 2919  $\text{cm}^{-1}$  remain nearly constant under all tested conditions fluctuating from 0.30 to 0.37. On the other hand, the ratio between the peaks at 1210  $\text{cm}^{-1}$  and 2919  $\text{cm}^{-1}$  increases progressively, reaching the maximum value when treating LDPE with the lcAlk\_3d secretome (Table 1). Moreover, this specific intensity ratio is 2.3-fold higher when compared to the C16\_3d condition, marking the day with the highest difference between lcAlk and C16 during this time-course experiment. Both lcAlk\_3d and C16\_3d were selected for multi-omics analysis. The lcAlk\_2d secretome, also selected for further analysis, exhibited significantly lower intensity ratios between the peaks at 1210  $\text{cm}^{-1}$  and 2919  $\text{cm}^{-1}$  compared to the lcAlk\_3d secretome (3.5-fold lower intensity ratio), suggesting that the microorganism adapted towards lcAlk breakdown after 3 days. A delayed response was observed in C16, with the intensity ratio peaking at day 4, yet remaining lower than that of lcAlk\_3d. These differences indicate that lcAlk\_3d secretome may be enriched with distinct and/or more abundant LDPE-converting enzymes. This contrasts with both C16\_3d and, to a greater extent, lcAlk\_2d secretomes, which served as comparative proxies in the subsequent differential analysis.

Similar studies have documented the capacity of various fungal species to induce chemical modifications in PE through microbial degradation, particularly detectable via FTIR spectroscopy

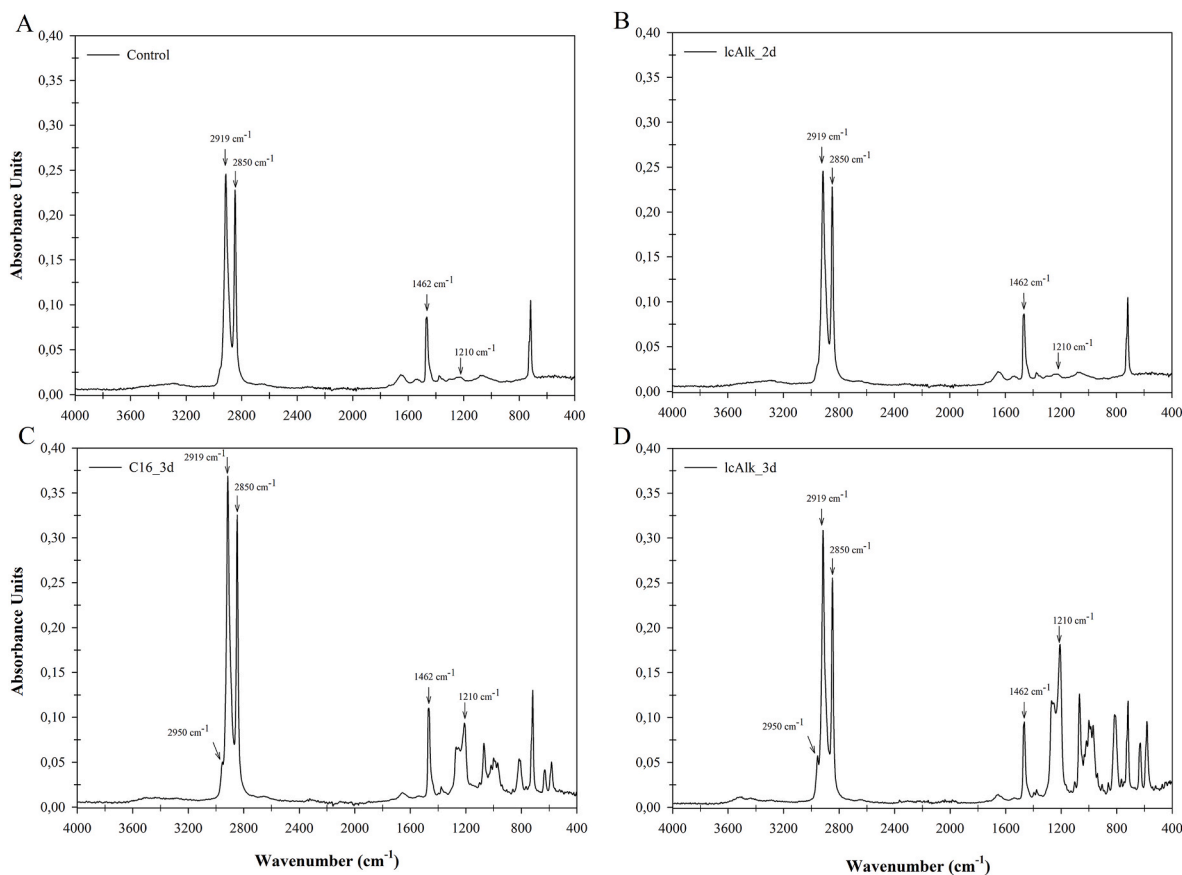


**Fig. 1.** ATR-FTIR spectrum of virgin LDPE powder (A) and LDPE powder after treatment with the secretome of *A. parasiticus* MM36, when grown in presence of lAlk for 2 days (B), and C16 (C) or lAlk (D) for 3 days, respectively.

**Table 1**

Calculated intensity ratios between characteristic PE peaks and newly formed on ATR-FTIR spectra.

| Sample  | Intensity ratio 1462 cm <sup>-1</sup> /2919 cm <sup>-1</sup> | Intensity ratio 1210 cm <sup>-1</sup> /2919 cm <sup>-1</sup> |
|---------|--|--|
| Control | 0.35   | 0.07   |
| lAlk_1d | 0.36   | 0.11   |
| lAlk_2d | 0.31   | 0.17   |
| lAlk_3d | 0.31   | 0.59   |
| lAlk_4d | 0.31   | 0.39   |
| C16_1d  | 0.37   | 0.13   |
| C16_2d  | 0.35   | 0.08   |
| C16_3d  | 0.30   | 0.26   |
| C16_4d  | 0.31   | 0.48   |

(Sathiyabama et al., 2024; Spina et al., 2021; Wróbel et al., 2023; Zhang et al., 2020a). As summarized in Table S1, fungi belonging predominantly to the phylum *Ascomycota* have demonstrated the ability to alter the molecular fingerprint of different PE substrates. According to previous reports, microbial treatment of PE leads to the formation of new functional groups, such as alcohols, esters, ethers, and carbonyls detected by FTIR, highlighting the potential of fungi in the degradation of recalcitrant polymers.

### 2.3. Secretomic analysis reveals strong substrate and time-dependent variability

We proceeded analyzing the secretomes of *A. parasiticus* MM36 grown under three selected conditions (lAlk\_2d, lAlk\_3d and C16\_3d) using label-free data-dependent LC-MS/MS proteomics in triplicates to identify enzymes facilitating lAlk assimilation and potentially

interacting with PE. As mentioned before, the assimilation of lower molecular weight alkanes from the water phase is feasible due to their solubility (Rojo, 2009), while lAlk assimilation requires extracellular oxyfunctionalization (Zadjelovic et al., 2022).

A total of 20.7 % of the MS/MS spectra were successfully matched to peptides in the protein database, resulting to the identification of 5230 peptides corresponding to 1096 proteins. On average, 25 % of the spectra analysed in an MS experiment can be identified, however this percentage is expected to drop when analysing the secretome instead of the whole proteome (Griss et al., 2016), as observed in previous studies (Pantelic et al., 2024). After applying a filter for proteins present in at least two replicates of any condition, 722 proteins were reliably quantified, with 34.6 % predicted to be extracellular compared to 10.0 % of the total proteome. The predominant enzyme group was oxidoreductases (140 proteins), followed by 74 proteins of unknown function. Forty-three of these uncharacterized proteins along with 38 other proteins in the secretomes are shorter than 300 amino acids and are classified as small secreted proteins (SSPs). The primary biological role of many SPPs in host-associated fungi like *A. parasiticus* MM36 is the interaction with the living host (Feldman et al., 2020).

Secretome profiles showed strong substrate- and time-dependent variability, with the lAlk\_3d condition displaying the richest secretome encompassing almost all quantified proteins. In contrast, the lAlk\_2d condition exhibited the fewest proteins, with only half of the total proteins observed across all conditions. Most differentially abundant proteins were induced in the lAlk\_3d secretomes, with 154 differing from lAlk\_2d and 7 from C16\_3d, 6 of which were common. This result aligns with the ATR-FTIR analysis, which showed maximal PE modification by lAlk\_3d secretomes and minimal activity in lAlk\_2d secretomes.

Differential analysis highlighted a predominance of hydrolytic

enzymes, including 15 peptidases, 16 glycoside hydrolases, 7 esterases, three phosphatases, one amidase, and one cysteinase. Six glycoside hydrolases contain carbohydrate-binding modules, and additional induced proteins included three carbohydrate-binding lectins and one LysM (lysine motif) domain-containing protein.

#### 2.4. Identification of potential plastizymes in *Aspergillus parasiticus* MM36 secretomes

We sought to identify enzymes potentially capable of oxidizing PE within the secretomes of *A. parasiticus* MM36. Multicopper oxidases (MCOs) constitute the AA1 CAZy family and contain laccases, ferroxidases and *Ascomycota* laccase-like enzymes (Levasseur et al., 2013). To date, two MCOs from *Rhodococcus opacus* R7 are the only isolated enzymes shown to oxidize PE and release a variety of alkanes and oxygenated hydrocarbons (Zampolli et al., 2023). Additionally, a MCO from *Parvibaculum lavamentivorans* degrades C19-C25 alkanes with a yield of more than 90% (Diefenbach et al., 2024). *A. parasiticus* MM36 genome encodes 15 MCOs, all of which contain the three characteristic

cupredoxin-like domains (IPR008972) and four MCOs were quantified in the secretomes. The AA1\_3 laccase-like RU639\_012907 was induced in lAlk\_3d compared to both lAlk\_2d and C16\_3d. Another MCO (RU639\_007412) was induced compared to lAlk\_2d and shares 94.6% amino acid identity with AFLA\_006190, one of the two MCOs upregulated during the degradation of PE by *A. flavus* PEDX3 (Zhang et al., 2020a).

Unspecific peroxygenases (UPOs) are extracellular heme proteins that catalyze various C-H oxyfunctionalization reactions using hydrogen peroxide as an oxygen donor (Faiza et al., 2019). UPO1 from *Agrocybe aegerita* hydroxylates linear alkanes up to C16 but is inactive on longer chains (Peter et al., 2011). MroUPO from the white-rot fungus *Marasmius rotula* initiates a cascade of mono- and di-terminal oxygenation reactions of dodecane (C12) and tetradecane (C14) to the corresponding carboxylic acids (Olmedo et al., 2016). UPOs are classified in InterPro as members of the chloroperoxidase protein family (IPR000028) (Paysan-Lafosse et al., 2023). The genome of *A. parasiticus* MM36 encodes five extracellular chloroperoxidases; among these only RU639\_007575 was detected in our experiment and was induced in

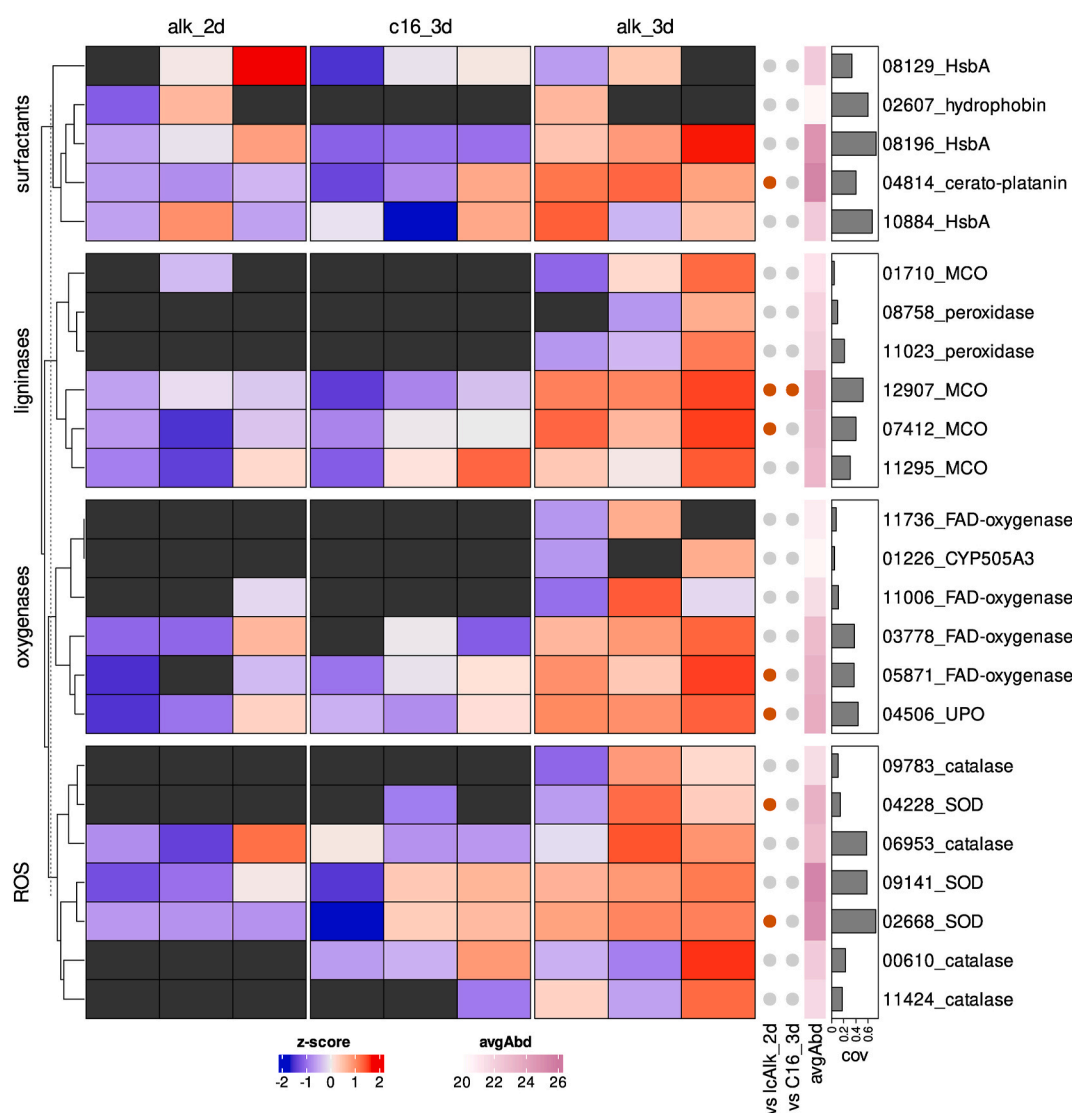


**Fig. 2.** Heatmap of z-scores of protein intensities for selected proteins; black color means not detected in the corresponding sample. Row clustering of each group is based on Euclidean distances of their z-scores. Protein accessions are shown without the RU639\_0 prefix. Proteins differentially abundant in lAlk\_3d compared to lAlk\_2d or C16\_3d are marked with an orange circle. peptide coverage: Number of detected peptides divided by number of theoretical tryptic peptides. protein intensity:  $\log_2$  of average protein intensity in lAlk\_3d. ROS: reactive oxygen species; MCO: multicopper oxidase; UPO: unspecific peroxygenase; SOD: superoxide dismutase; HsbA: hydrophobic surface-binding protein A. (For interpretation of the references to color in this figure legend, the reader is referred to the Web version of this article.)

lcAlk\_3d secretomes. RU639\_007575 is a short UPO of 27.5 kDa that contains the characteristic PCP (Proline-Cysteine-Proline) amino acid motif for heme-binding, as well as the EHD (Glutamate-Histidine-Aspartate) motif. The latter is a conserved signature for UPOs like MroUPO (Faiza et al., 2019). The most studied lcAlk oxidases, able to hydroxylate alkanes up to C36 to their primary alcohols, are the bacterial flavin-dependent monooxygenases named LadA and Alma (Feng et al., 2007; W. Wang & Shao, 2014). LadA belongs to the luciferase family (IPR016215), while Alma is part of the FAD-binding monooxygenase family (IPR051820). However, enzymes from these families in *A. parasiticus* MM36 are intracellular and were not detected in the secretomes. In contrast, four flavin-dependent monooxygenases belonging to a distinct FAD-binding superfamily (IPR036318) were identified in the secretomes, with RU639\_005614 being differentially abundant in lcAlk\_3d compared to lcAlk\_2d (Fig. 2). Another monooxygenase of interest is CYP505A3, secreted exclusively in lcAlk\_3d. Members of the CYP505 family of the cytochrome P450 monooxygenases are considered sub-terminal fatty acid hydroxylases, while CYP505E3 from *A. terreus* catalyses also the regioselective in-chain hydroxylation of C10-C16 n-alkanes (Maseme et al., 2020).

Alkane hydroxylases overcome the low chemical reactivity of the alkanes by generating reactive oxygen species (ROS) (Rojo, 2009), a strategy also proposed for PE oxidation (Zadjelovic et al., 2022). ROS could also assist the action of the mentioned secreted monooxygenases. Additionally, ROS activate oxidative enzymes such as peroxidases. A bacterial peroxidase degrades polystyrene, an aromatic polymer with a C-C backbone similar to PE that generates water soluble products in the presence of H<sub>2</sub>O<sub>2</sub> (Nakamiya et al., 1997). The lcAlk\_3d secretomes contain two lignin peroxidases undetected in other conditions, a member of the AA2 CAZY family (RU639\_011023), and a DyP-type peroxidase (RU639\_008758). Interestingly, three superoxide dismutases were also induced in lcAlk\_3d compared to lcAlk\_2d (Fig. 2). These enzymes help control ROS levels, protecting the fungus from oxidative stress and preventing enzyme inhibition (Zhang et al., 2020b). While catalases, which also control ROS levels, were quantified at similar levels across all conditions, the induction of a superoxide dismutase rather than catalases has also been observed in *Alcanivorax* sp. 24 when exposed to pristine LDPE (Zadjelovic et al., 2022). Additionally, one thioredoxin, a protein associated with oxidative stress, and one thioredoxin reductase were detected only in the secretomes of lcAlk\_3d.

Beyond oxidative enzymes, proteins involved in hydrocarbon uptake in fungi include those that modify the hydrophobicity of the cell surface or the hydrocarbon itself to enable cell adhesion. Hydrophobins promote sorption by increasing the cell surface hydrophobicity and constitute the IPR001338 Interpro family. This is exemplified in the fungus *Paecilomyces lilacinus*, which grows on C16 producing hydrophobins in solid-state cultures (Vigueras et al., 2014). The genome of *A. parasiticus* MM36 encodes three extracellular hydrophobins, but only the hydrophobin RU639\_002607, an ortholog of RolA from *Aspergillus oryzae*, was detected by MS in two replicates of lcAlk\_2d and one replicate of lcAlk\_3d (Fig. 2). RolA is a hydrophobin that is known in literature to enhance PET degradation underpinning its potential for PE modification (Puspitasari et al., 2021).

Additionally, the secretomes contained three members of Hydrophobic surface-binding protein A (HsbA) family (IPR021054), with similar abundance across conditions (Fig. 2). One of these contains a GPI-anchor that keeps it attached to the cell wall. A HsbA from the pathogen *Penicillium marneffei* binds long-chain fatty acids and stores them in the cell wall for nutrient starvation resilience (Liao et al., 2010). RU639\_010884 is orthologous to a HsbA from *A. oryzae* that binds hydrophobic polybutylene succinate-co-adipate (PBSA) promoting its degradation via a cutinase (Shinsaku et al., 2006). Cerato platanins are another protein family with surfactant properties that reduce the surface hydrophobicity of plastics (Renwei et al., 2020). *A. parasiticus* genome encodes two cerato platanins, one of which was constitutively secreted across all samples.

## 2.5. Transcriptomic profiling during alkane assimilation

To study the response of *A. parasiticus* MM36 to lcAlk and C16, and to identify the biological processes involved in their assimilation, we conducted RNA-seq at the same three conditions as secretomics analysis. After filtering out low-count genes, 11,964 genes were retained for differential expression analysis and the subsequent enrichment analyses. Overall, gene expression changes between the lcAlk timepoints were modest, with fewer than 250 genes differentially expressed, contrasting with the more pronounced variations observed at the secretome level. Conversely, numerous genes displayed differential expression when comparing both lcAlk timepoints to C16\_3d, with approximately 1000 genes upregulated in lcAlk conditions and nearly double in C16\_3d.

Genes were mapped to gene ontology (GO) terms using InterProScan, and differentially expressed genes were tested for the enrichment of biological processes and molecular functions with GOATOOLS (Klopfenstein et al., 2018). Analysis comparing lcAlk\_2d with C16\_3d revealed an enrichment of genes associated with transmembrane transport processes, predominantly involving the Major Facilitator Superfamily (MFS) and ATP-binding Cassette (ABC) transporter families (Fig. 3). Similarly, the majority of *Rhodococcus ruber* transporters upregulated in the presence of PE were MFS and ABC transporters (Gravouil et al., 2017), while in *Yarrowia lipolytica*, an ABC transporter is involved in the uptake of C16 (Thevenieau et al., 2007).

Alkane metabolism involves their conversion to alcohols and carboxylic acids, and their subsequent catabolism through the well-studied fatty acid metabolism/ $\beta$ -oxidation pathway (Montazer et al., 2020). Two relevant, enriched processes are monocarboxylic acid metabolism and its child term, fatty acids metabolism (Fig. 3). Their upregulated genes include polyketide and fatty acid synthases, fatty acid desaturases, dehydrogenases, kinases and other transferases. Another interesting, enriched function is anion binding, particularly the binding of flavin mononucleotide (FMN), since many oxidases involved in alkane and fatty acid oxidation are flavoenzymes. Among these are the previously mentioned bacterial lcAlk hydroxylases LadA and Alma (Feng et al., 2007; W. Wang & Shao, 2014). The genome of *A. parasiticus* encodes five luciferase-like monooxygenases with more than 40 % amino acid identity with LadA, consistent with finding in *A. flavus* (Perera et al., 2022) and one of them (RU639\_010847) was upregulated in lcAlk\_2d compared to C16\_3d. Similarly, one of the seven genes classified within the same flavin monooxygenase family (IPR051820) as Alma was upregulated in both lcAlk days.

GO enrichment in lcAlk\_3d compared to C16\_3d mirrored the enrichment of binding functions and oxidoreductase activities as in lcAlk\_2d but exhibited unique differences. Notably, transmembrane and transport activities seen in lcAlk\_2d were absent, replaced by an increase in metabolic and biosynthetic processes related to carboxylic acids and other small molecules. Of the 26 upregulated genes involved in carboxylic acid biosynthesis, 14 were also upregulated in lcAlk\_2d. The accumulation of stable carboxylic acids results from the further oxidation of the generated alcohols, aldehydes and ketones during alkane metabolism (Hakkarainen & Albertsson, 2004). The use of alkanes for both energy generation and the biosynthesis of molecules such as lipids has been documented in entomopathogenic fungi (Napolitano & Juárez, 1997). In conclusion, the induction of transmembrane and transport activities needed for alkane internalization during the early response (lcAlk\_2d) is followed by their incorporation into the metabolic processes of *A. parasiticus* MM36, as reflected in the shift towards biosynthetic and metabolic activities in lcAlk\_3d.

The analysis of genes upregulated when the fungus was grown on C16 displayed a different profile. Although 1800 genes were upregulated compared to lcAlk\_2d, their high heterogeneity led to no enriched GO terms. However, when compared to lcAlk\_3d, C16\_3d exhibited strong enrichment of hydrolase activities, highlighting an abundance of glucoside hydrolases involved in carbohydrate metabolism, as well as peptidases, amidases, and esterases. While the strong enrichment of

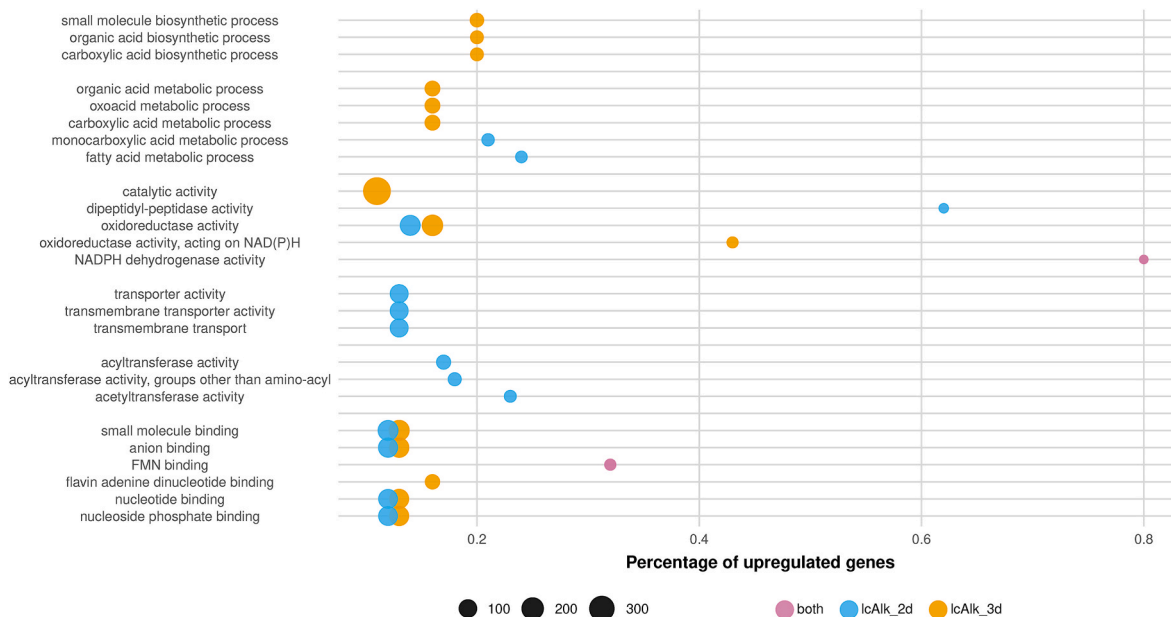


**Fig. 3.** Bubble plot of gene ontology (GO) terms enriched in lCAlk\_2d, lCAlk\_3d or both lCAlk days vs C16\_3d. Bubble size is proportional to the number of upregulated genes.

peptidases and amidases lacks a clear explanation, the esterases can be linked to the action of Baeyer-Villiger monooxygenases (BVMOs). BVMOs catalyze the conversion of a ketone to an ester, a reaction useful in case of sub-terminal alkane oxidation. Two BVMOs were upregulated in C16\_3d compared to both lCAlk timepoints, while the other five displayed consistently low expression across all conditions. All seven BVMOs of *A. parasiticus* MM36 have orthologs in *A. flavus* with more than 94 % sequence identity, but these orthologs have demonstrated activity only up to n-C12 (Ferroni et al., 2014). This suggests that sub-terminal oxidation is more likely to occur in C16\_3d rather than lCAlk, differing from the bacterium *Thalassolituus oleivorans* MIL-1, which uses terminal oxidation for C14, but shifts to sub-terminal oxidation for longer alkanes (Gregson et al., 2018).

## 2.6. Discrepancy between transcriptomic and secretomic profiles

To assess the regulation of differentially abundant proteins at the transcriptome level we examined the overlap between the two datasets. Out of 154 proteins induced in lCAlk\_3d versus lCAlk\_2d, only seven of the corresponding genes were differentially regulated, and most of these exhibited the opposite trend — being downregulated in lCAlk\_3d. A comprehensive meta-analysis in yeast estimated that mRNA abundance explains only 37–56 % of the variance in protein abundance due to a variety of post-transcriptional regulation modes including translation and protein modifications (Ho et al., 2018). In our study, the expected correlation is likely even lower, since transcriptomic and proteomic data were obtained from different compartments — total cellular RNA versus proteins secreted in the culture supernatant — adding an extra layer of divergence. Similar findings have been reported in *Aspergillus fumigatus*, where weak correlation between transcriptomic and secretomic profiles was observed (Adav et al., 2010; de Gouvêa et al., 2018). Gouvêa et al. notably attributed part of this discrepancy to time lags between transcription, translation, and eventual secretion.

Focusing on enzyme families highlighted in the secretomic analysis, we observed transcriptional upregulation of MCOs in lCAlk samples; four out of the 14 MCO expressed genes, including RU639\_012907 (also differentially abundant in the lCAlk\_3d secretome), were upregulated in both lCAlk days compared to C16\_3d. Additionally, four MCOs were upregulated in one of the lCAlk days versus C16\_3d. In contrast, the RU639\_008758 lignin peroxidase was upregulated in C16\_3d compared

to lCAlk\_3d, while RU639\_011023 peroxidase displayed similar expression levels across all conditions. Both transcribed UPOs, including the secreted RU639\_004506, were downregulated in lCAlk\_3d relative to C16\_3d.

## 2.7. Proposed mechanism of alkane assimilation by *A. parasiticus* MM36

Integrating the data from transcriptomic and secretomic analyses, we propose a potential mechanism for lCAlk functionalization, uptake and assimilation by *A. parasiticus* MM36 (Fig. 4). A secreted hydrophobin, a cerato platanin and three HsbA may act as surfactants to facilitate the initial enzyme and cell sorption to lCAlk. A variety of secreted enzymes that could oxygenate the alkanes is being secreted. Lignin active enzymes, including 4 MCOs and two peroxidases can act in an unspecific manner potentially generating various oxygenated products and causing chain scission. Oxygenases including an UPO, four flavin-dependent oxygenases and a CYP505 hydroxylase can introduce terminal, sub-terminal, or di-hydroxyl groups into the alkanes, initiating their transformation into more reactive forms. These reactions are likely facilitated by ROS, which provide the necessary oxygen atoms. To mitigate potential ROS-related damage, *A. parasiticus* MM36 appears to produce ROS-controlling enzymes, including superoxide dismutases and catalases. Alcohols generated through these reactions could be further converted to aldehydes or ketones by five alcohol dehydrogenases, while three aldehyde dehydrogenases can convert the aldehydes to carboxylic acids. The secreted surfactants may interact with the produced hydrocarbons and facilitate cell adhesion and subsequent uptake through the cell wall and the membranes. This uptake could involve ABC and other membrane transporter families. While the proposed mechanism is based on the assimilation of lCAlk, the secretomic activity of *A. parasiticus* MM36 has been shown to modify LDPE under similar conditions. This connection is further supported by growing evidence that alkane-degrading microbes also have the potential to degrade PE, as reported in the Introduction paragraph. Both substrates share key physicochemical traits; they are hydrophobic, consist of a carbon-carbon backbone, lack functional groups and require extracellular oxygen functionalization.

Once inside the cell, these compounds can be directed toward catabolic or biosynthetic processes. In case of sub-terminal oxidation, the seven intracellular BVMOs may catalyze the conversion of ketones into

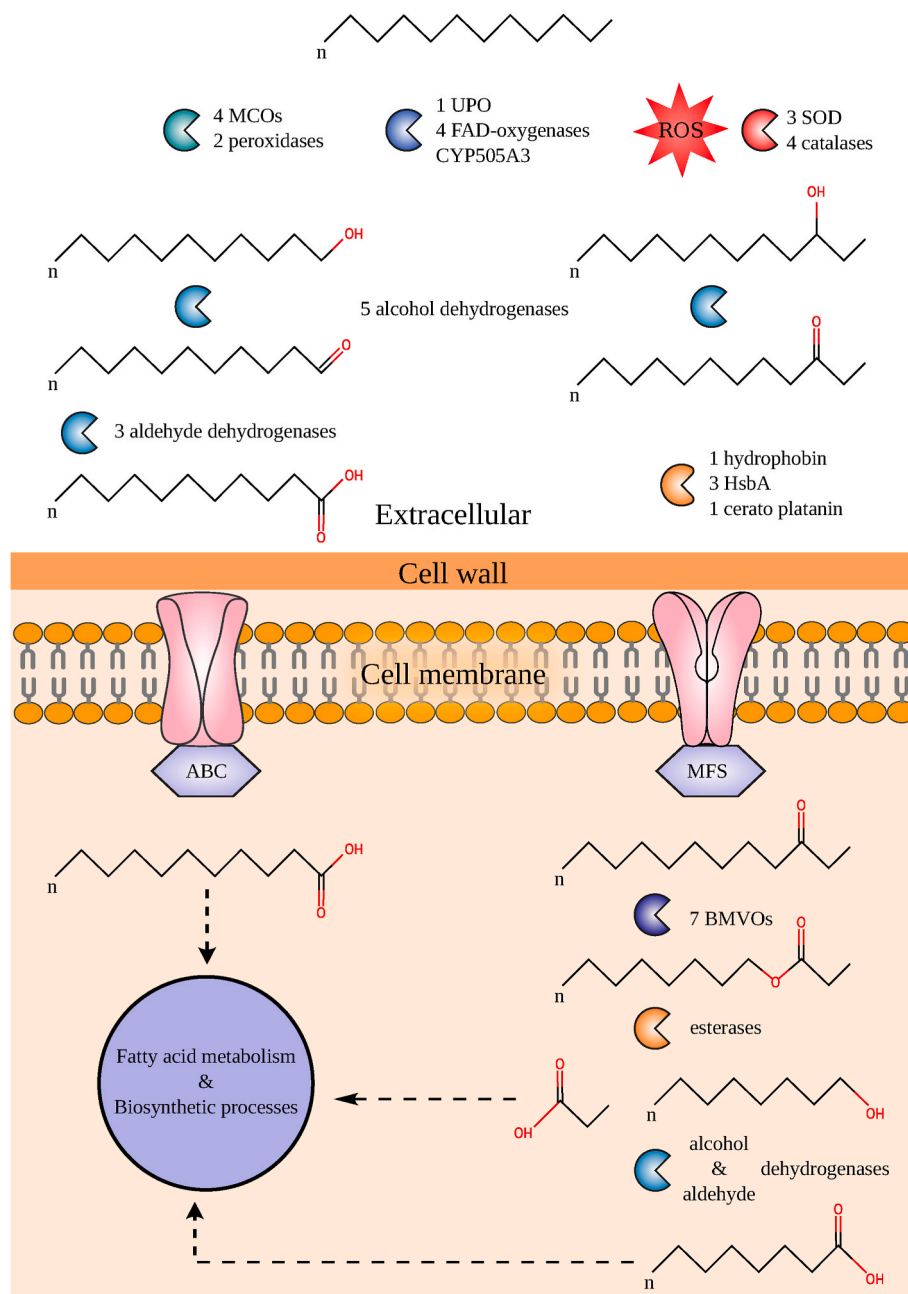


Fig. 4. Proteomics- and transcriptomics-informed potential mechanism of alkane assimilation by *A. parasiticus* MM36. ROS: reactive oxygen species; MCO: multi-copper oxidase; UPO: unspecific peroxygenase; SOD: superoxide dismutase; HsbA: hydrophobic surface-binding protein A; BMVO: Baeyer-Villiger mono-oxygenase.

esters, which could be hydrolyzed by a cascade of intracellular esterases, resulting in smaller chain carboxylic acids. The resulting fatty acids are likely directed to the well-studied  $\beta$  oxidation pathway for energy generation or to biosynthetic pathways for lipid and small molecule production.

### 3. Materials and methods

#### 3.1. Genome sequencing and analysis

DNA extraction from *A. parasiticus* MM36 was performed as described in the Supplementary Material. A 350-bp insert size library was prepared and sequenced in paired-end mode (read length, 150 bp) by Novogene Europe on a NovaSeq 6000 instrument. Adapter sequences were removed (at an alignment score above 7, allowing 2 mismatches),

and bases with a quality score below 10 and below an average of 20 on a 5-bp window were trimmed using Trimmomatic v.0.39 (Bolger et al., 2014). Reads smaller than 50 bases or with no pair (singletons) were discarded. Reads mapping to viral and bacterial genomes were removed with Kraken2 v.0.8 (Wood et al., 2019), with a confidence score of 0.7. *De novo* genome assembly was performed with Spades v3.15.4 with the isolate parameter (Prjibelski et al., 2020). Genome completeness was assessed with BUSCO v5.1.2 using the *Eurotiales* phylum single-copy orthologs (Manni et al., 2021).

Repeats were *de novo* identified with RepeatModeler v2.0 and LTRharvest (Ellinghaus et al., 2008) and were then searched against SwissProt after excluding transposases with an E-value threshold of 1e-10. Repeats aligned with protein-coding genes are removed with ProtExcluder v1.2. Next, repeat sequences were converted to lowercase letters (soft-masking) for downstream gene prediction using

RepeatMasker v4.1.2 with the library of de novo identified repeats and the fungal repeat elements of Repbase 2017 and 2019 (Tarailo-Graovac & Chen (2009).

Gene prediction was performed with BRAKER v3.0.3 (Gabriel et al., 2024) using the fungal partition of orthoDB v11 (Kuznetsov et al., 2023) and mapped RNAseq reads. The predicted genes and isoforms were reduced with TSEBRA (Gabriel et al., 2021) and the gene models were supplemented to MAKER v2.31.11 (Holt & Yandell, 2011) along with a Trinity assembly (Haas et al., 2013) of the RNA-Seq data to append the untranslated regions (UTRs) to the BRAKER gene models.

Proteins were functionally annotated with UniFIRE v2023.3. Gene and product names were assigned via UniFIRE and BLAST to SwissProt after filtering the alignments with Haas et al. criteria (Haas et al., 2011). CAZymes were identified with run\_dbcan v4.1.4 (Zheng et al., 2023). HMMER3 alignments were filtered with an e-value of  $1e^{-17}$  and coverage 45 %. Proteins annotated only with DIAMOND were rerun in ultra-sensitive mode and filtered for 95 % coverage of both the query and subject sequence following the latest recommendations (Drula et al., 2022). Transporters were searched with BlastP and hmmsearch against TCDB downloaded in January 2024 (Saier Jr et al., 2021). Blast alignments were filtered for 70 % coverage and 30 % percent identity and hmmsearch for bitscore 100. Extracellular proteins were predicted with UniFIRE and DeepLoc2 (Thumuluri et al., 2022) or SignalP6 (Teufel et al., 2022) in the lack of transmembrane helices in the mature protein. Proteins with a signal peptide were searched for glycosylphosphatidylinositol (GPI) anchoring signal with NetGPI v1.1 (Gislason et al., 2021).

### 3.2. Phylogenetic analysis

To classify *A. parasiticus* MM36 at the species level, all available proteomes included in a previous phylogenetic analysis of the *Aspergillus Flavi* section (Kjærboelling et al., 2020) were retrieved from MycoCosm (Grigoriev et al., 2014). Additionally, the reference genome of *A. sojae* SMF134 was downloaded from GenBank (accession GCA\_008274985.1) and genes were predicted with GeneMark-ES v4.71 adapted for fungal genomes (Ter-Hovhannisyann et al., 2008).

Steenwyk et al. (2024) generated profile Hidden Markov Models (HMMs) for single-copy orthologs of the *Aspergillus* genus. These HMMs were filtered for a length between 100 and 1000 amino acids and then 200 HMMs were randomly subsampled. The resulting HMMs were used to identify single-copy orthologs in the proteomes using orthofisher v1.0.5 (Steenwyk & Rokas, 2021) and orthologs were aligned with mafft v7.490 (Katoh & Standley, 2013). Maximum-Likelihood phylogenetic analysis was performed with IQ-TREE v2.3.6 with an edge-linked fully-partitioned model (Minh, Schmidt, et al., 2020). Node support was calculated using 1000 ultrafast bootstraps and 1000 iterations of the SH-like approximate likelihood ratio test (Hoang et al., 2018). We calculated gene (gCF) and site concordance factors (sCF) by comparing single-gene trees to the concatenated tree (Minh, Hahn, et al., 2020).

### 3.3. Induction of PE-transforming enzymes and sample preparation for multi-omics analyses

Induction of potential PE-transforming enzymes was carried out in liquid cultures using mineral medium (MM) either supplemented with C16 or a lAlk mixture. The growth media were prepared following the protocol described in a previous study (Taxeidis et al., 2023). Cultures were incubated at 27 °C, under continuous stirring at 120 rpm for 4 days. Each day, the mycelial biomass and the culture supernatant were collected separately. The fungal biomass was harvested under vacuum and washed with ultrapure water under aseptic conditions and immediately flash-frozen using liquid nitrogen. The culture supernatant was dialyzed overnight against 20 mM Tris-HCl buffer (pH 7.0) and freeze-dried under vacuum. After selecting the optimal time points the

respective biomass samples were sent to Novogene B.V. (Netherlands) for RNA extraction, while corresponding supernatants were sent to the VIB Proteomics Core facility (Ghent, Belgium) for peptide purification and LC-MS/MS analysis. Both analyses were performed using triplicate biological samples.

The optimal time points for transcriptomics and proteomics analysis were determined by evaluating the ability of culture supernatants to effectively modify LDPE structure. Specifically, following the methodology detailed in a previous study (Taxeidis et al., 2023), each of the culture supernatants collected daily was tested for its ability to degrade LDPE powder. In this procedure, 50 mg of LDPE powder was incubated with 50 mL of the culture supernatant at 30 °C with continuous stirring at 160 rpm for 4 days. After incubation, the plastic powder was removed, washed with 2 % (w/v) sodium dodecyl sulfate (SDS), and dried. The properties of LDPE were then analysed using Attenuated total reflectance-Fourier transform infrared spectroscopy (ATR-FTIR) to detect changes in the polymer's molecular structure, following the same protocol as those mentioned in a previous study (Taxeidis et al., 2023).

### 3.4. LC-MS/MS analysis of the secretomes

Sample preparation, trypsin digestion and peptide elution are described in the Supplementary Material. One  $\mu$ L of each sample was injected for LC-MS/MS analysis on an Ultimate 3000 RSLCnano system in-line connected to a Q Exactive HF Biopharma mass spectrometer (Thermo). The peptides were separated on a 250 mm Aurora Ultimate, 1.7  $\mu$ m C18, 75  $\mu$ m inner diameter (Ionopticks) kept at a constant temperature of 45 °C. The mass spectrometer was operated in data-dependent mode, automatically switching between MS and MS/MS acquisition for the 12 most abundant ion peaks per MS spectrum. Full-scan MS spectra (375–1500 m/z) were acquired at a resolution of 60,000 in the Orbitrap analyser after accumulation to a target value of 3,000,000. The 12 most intense ions above a threshold value of 15,000 were isolated with a width of 1.5 m/z for fragmentation at a normalized collision energy of 28 % after filling the trap at a target value of 100,000 for maximum 120 ms. QCloud has been used to control instrument longitudinal performance during the project (Chiva et al., 2018).

### 3.5. Processing of the LC-MS/MS data

The raw data were searched together using the nf-core/quantms v1.3.0dev (Dai et al., 2024) pipeline of the nf-core collection of workflows (Ewels et al., 2020) against the proteome of *A. parasiticus* MM36 and a proteomics contaminant library (Frankenfield et al., 2022). The pipeline was executed with Nextflow v24.04.2 (Di Tommaso et al., 2017), utilizing reproducible software environments from the Bioconda (Grüning et al., 2018) and Biocontainers (da Veiga Leprevost et al., 2017) projects. Precursor mass tolerance was set to 15 ppm based on Param-Medic (May et al., 2017) and fragment mass tolerance was set to 0.02 Da. Trypsin cleavage was allowed a maximum of two missed cleavages. The peptide identification step was performed with Comet, MS-GF+ and SAGE (Eng et al., 2013; Kim & Pevzner, 2014; Lazear, 2023), with search engine results rescored by MS2Rescore (Declercq et al., 2022). Variable modifications were set to oxidation of methionine and tryptophan, acetylation of protein N-termini, deamidation of asparagine and N-terminal glutamine conversion to pyroglutamic acid and ammonia loss of cysteine. Carbamidomethylation of cysteine residues was set as a fixed modification. These modifications were determined after an open search of the raw data using Fragpipe with default settings (Geiszler et al., 2021; Kong et al., 2017).

The peptide level intensities were imported in the prolfqua package (Wolski et al., 2023),  $\log_2$  transformed and robust z-score scaled. Protein intensities were estimated from peptide intensities using Tukey's median polish (TMP). However, TMP summarization creates artifacts in cases where all peptides of a protein are detected uniquely in single samples, yielding misleading uniform protein intensities across all

samples. This phenomenon is previously reported in microarray data summarization (Giorgi et al., 2010). For proteins affected by this artifact, median summarization of the top three peptides was employed instead. Subsequently, only reliably quantified proteins present in at least two biological replicates of one condition were retained for downstream analysis. Differential protein abundance was tested using the empirical Bayes approach with imputation of missing values as implemented in prolfqua.

### 3.6. Transcriptome analysis during alkane assimilation

Total RNA was extracted from each timepoint in triplicates by Novogene, the polyA + fraction was purified, and libraries were constructed with the Novogene NGS RNA Library Prep Set (PT042) kit and sequenced in paired-end mode on a NovaSeq 6000. One C16 sample with a RIN value of 3.7 was discarded leaving this condition with two replicates. Raw data were processed using *nf-core/rnaseq* v3.10.1 (Patel et al., 2024) of the *nf-core* collection of workflows (Ewels et al., 2020) at the high-performance computing bioinformatics platform of HCMR (Crete, Greece) (Zafeiropoulos et al., 2021). Raw counts were loaded in edgeR v3.43.4 and were normalized using the TMM normalization (Robinson et al., 2010). Based on previous research (Chen et al., 2016) genes with low expression were excluded. Specifically, only genes with more than 10/L reads, where L = 16.66 represents the median library size in millions, in at least two replicates of any condition were retained for downstream analysis. Differential expression (DE) was tested with the edgeR-exact test following recommendations for few replicates (Schurch et al., 2016). The p-value was adjusted with the Benjamini-Hochberg (B-H) correction and corresponds to an FDR of 5%. Gene ontology (GO) enrichment analysis was performed using goatoools v1.3.1 (Klopfenstein et al., 2018) with the go-basic.obo release 2023-04-01 to test for the overrepresentation of GO terms among differentially expressed genes. Fisher's exact test was used with 5% B-H FDR and GO terms were derived from the Interproscan annotations.

### CRedit authorship contribution statement

**Romanos Siaperas:** Writing – review & editing, Writing – original draft, Visualization, Validation, Methodology, Investigation, Formal analysis, Data curation. **George Taxeidis:** Writing – original draft, Visualization, Methodology, Investigation, Formal analysis. **Anastasia Gioti:** Resources, Methodology. **Efstratios Nikolaivits:** Writing – review & editing, Validation, Supervision, Methodology, Investigation, Conceptualization. **Evangelos Topakas:** Writing – review & editing, Validation, Supervision, Resources, Project administration, Funding acquisition, Conceptualization.

### Funding

This research was funded by the Hellenic Foundation for Research and Innovation (H.F.R.I.) under the “2nd Call for H.F.R.I. Research Projects to support Faculty Members and Researchers” (Project Number: 03061, PlastOmics).

### Declaration of competing interest

The authors declare the following financial interests/personal relationships which may be considered as potential competing interests: George Taxeidis reports financial support was provided by Hellenic Foundation for Research and Innovation. Evangelos Topakas reports financial support was provided by Hellenic Foundation for Research and Innovation. If there are other authors, they declare that they have no known competing financial interests or personal relationships that could have appeared to influence the work reported in this paper.

### Acknowledgments

The authors would like to thank the VIB Proteomics Core for the contribution regarding the mass spectrometry-based proteomics experiments (EPIC-XS, project number 823839, funded by the Horizon 2020 programme of the European Union). This research was supported in part through computational resources provided by IMBBC (Institute of Marine Biology, Biotechnology and Aquaculture) of the HCMR (Hellenic Centre for Marine Research). The authors thank Professor Stamatina Vouyiouka for providing equipment for the Attenuated total reflectance-Fourier transform infrared spectroscopy (ATR-FTIR) analysis.

### Appendix A. Supplementary data

Supplementary data to this article can be found online at <https://doi.org/10.1016/j.envpol.2025.126386>.

### Data availability

The Whole Genome Shotgun project has been deposited at DDBJ/ENA/GenBank under the accession JAWDVE000000000. The transcriptomic RNA-seq data have been deposited to the NCBI Gene Expression Omnibus (GEO) database with the dataset identifier GSE282836. The mass spectrometry proteomics data have been deposited to the ProteomeXchange Consortium via the PRIDE (Perez-Riverol et al., 2022) partner repository with the dataset identifier PXD058271 and 10.6019/PXD058271. Code for the transcriptomic and proteomic analysis is available in GitHub ([https://github.com/Roman-Si/Asp-parasiticus\\_alkane\\_multiomics](https://github.com/Roman-Si/Asp-parasiticus_alkane_multiomics)). The ATR-FTIR data will be made available on request.

### References

- Adav, S.S., Li, A.A., Manavalan, A., Punt, P., Sze, S.K., 2010. Quantitative iTRAQ secretome analysis of *Aspergillus niger* reveals novel hydrolytic enzymes. *J. Proteome Res.* 9 (8), 3932–3940. <https://doi.org/10.1021/pr100148j>.
- Al-Hawash, A.B., Zhang, J., Li, S., Liu, J., Ghalib, H.B., Zhang, X., Ma, F., 2018. Biodegradation of n-hexadecane by *Aspergillus* sp. RFC-1 and its mechanism. *Ecotoxicol. Environ. Saf.* 164, 398–408. <https://doi.org/10.1016/j.ecoenv.2018.08.049>.
- Bolger, A.M., Lohse, M., Usadel, B., 2014. Trimmomatic: a flexible trimmer for illumina sequence data. *Bioinformatics* 30 (15), 2114–2120. <https://doi.org/10.1093/bioinformatics/btu170>.
- Caleb, W., Max, M., Bindica, P., Christopher, C., Ryan, M., O, O.I., Seunghyun, R., Bamin, K., J, G.R., Siris, L., T, T.C., 2023. Proteomes reveal metabolic capabilities of *Yarrowia lipolytica* for biological upcycling of polyethylene into high-value chemicals. *mSystems* 8 (6), e00741. <https://doi.org/10.1128/msystems.00741-23>.
- Chamas, A., Moon, H., Zheng, J., Qiu, Y., Tabassum, T., Jang, J.H., Abu-Omar, M., Scott, S.L., Suh, S., 2020. Degradation rates of plastics in the environment. *ACS Sustain. Chem. Eng.* 8 (9), 3494–3511. <https://doi.org/10.1021/acssuschemeng.9b06635>.
- Chen, Y., Lun, A.T.L., Smyth, G.K., 2016. From reads to genes to pathways: differential expression analysis of RNA-Seq experiments using Rsubread and the edgeR quasi-likelihood pipeline [version 2; peer review: 5 approved]. *F1000Research* 5 (1438). <https://doi.org/10.12688/f1000research.8987.2>.
- Chiva, C., Olivella, R., Borràs, E., Espadas, G., Pastor, O., Solé, A., Sabidó, E., 2018. QCloud: a cloud-based quality control system for mass spectrometry-based proteomics laboratories. *PLoS One* 13 (1), e0189209. <https://doi.org/10.1371/journal.pone.0189209>.
- da Veiga Leprevost, F., Grüning, B.A., Alves Afritos, S., Röst, H.L., Uszkoreit, J., Bartsch, H., Vaudel, M., Moreno, P., Gatto, L., Weber, J., Bai, M., Jimenez, R.C., Sachsenberg, T., Pfeuffer, J., Vera Alvarez, R., Griss, J., Nesvizhskii, A.I., Perez-Riverol, Y., 2017. BioContainers: an open-source and community-driven framework for software standardization. *Bioinformatics* 33 (16), 2580–2582. <https://doi.org/10.1093/bioinformatics/btx192>.
- Dai, C., Pfeuffer, J., Wang, H., Zheng, P., Käll, L., Sachsenberg, T., Demichev, V., Bai, M., Kohlbacher, O., Perez-Riverol, Y., 2024. Quantms: a cloud-based pipeline for quantitative proteomics enables the reanalysis of public proteomics data. *Nat. Methods* 21 (9), 1603–1607. <https://doi.org/10.1038/s41592-024-02343-1>.
- de Gouveia, P.F., Bernardi, A.V., Gerolamo, L.E., de Souza Santos, E., Riano-Pachón, D.M., Uyemura, S.A., Dinamarco, T.M., 2018. Transcriptome and secretome analysis of *Aspergillus fumigatus* in the presence of sugarcane bagasse. *BMC Genom.* 19 (1), 232. <https://doi.org/10.1186/s12864-018-4627-8>.
- de Vries, R.P., Riley, R., Wiebenga, A., Aguilar-Osorio, G., Amillis, S., Uchima, C.A., Anderlüh, G., Asadollahi, M., Askin, M., Barry, K., Battaglia, E., Bayram, Ö.,

- Benocci, T., Braus-Stromeyer, S.A., Caldana, C., Cánovas, D., Cerqueira, G.C., Chen, F., Chen, W., et al., 2017. Comparative genomics reveals high biological diversity and specific adaptations in the industrially and medically important fungal genus *Aspergillus*. *Genome Biol.* 18 (1). <https://doi.org/10.1186/s13059-017-1151-0>.
- Declercq, A., Bouwmeester, R., Hirschler, A., Carapito, C., Degroev, S., Martens, L., Gabriels, R., 2022. MS2Rescore: data-driven rescoring dramatically boosts immunopeptide identification rates. *Mol. Cell. Proteomics* 21 (8), 100266. <https://doi.org/10.1016/j.mcpro.2022.100266>.
- Di Tommaso, P., Chatzou, M., Floden, E.W., Barja, P.P., Palumbo, E., Notredame, C., 2017. Nextflow enables reproducible computational workflows. *Nat. Biotechnol.* 35 (4), 316–319. <https://doi.org/10.1038/nbt.3820>.
- Diefenbach, T., Sumetzberger-Hasinger, M., Braunschmid, V., Konegger, H., Heipieper, H.J., Guebitz, G.M., Lackner, M., Ribitsch, D., Loibner, A.P., 2024. Laccase-mediated degradation of petroleum hydrocarbons in historically contaminated soil. *Chemosphere* 348, 140733. <https://doi.org/10.1016/j.chemosphere.2023.140733>.
- Drula, E., Garron, M.L., Dogan, S., Lombard, V., Henrissat, B., Terrapon, N., 2022. The carbohydrate-active enzyme database: functions and literature. *Nucleic Acids Res.* 50 (D1), D571–D577. <https://doi.org/10.1093/nar/gkab1045>.
- Ellinghaus, D., Kurtz, S., Willhoeft, U., 2008. LTRharvest, an efficient and flexible software for de novo detection of LTR retrotransposons. *BMC Bioinf.* 9. <https://doi.org/10.1186/1471-2105-9-18>.
- Eng, J.K., Jahan, T.A., Hoopmann, M.R., 2013. Comet: an open-source MS/MS sequence database search tool. *Proteomics* 13 (1), 22–24. <https://doi.org/10.1002/pmic.201200439>.
- Ewels, P.A., Peltzer, A., Fillinger, S., Patel, H., Alneberg, J., Wilm, A., Garcia, M.U., Di Tommaso, P., Nahnsen, S., 2020. The nf-core framework for community-curated bioinformatics pipelines. *Nat. Biotechnol.* 38 (3), 276–278. <https://doi.org/10.1038/s41587-020-0439-x>.
- Faiza, M., Huang, S., Lan, D., Wang, Y., 2019. New insights on unspecific peroxygenases: superfamily reclassification and evolution. *BMC Evol. Biol.* 19 (1), 76. <https://doi.org/10.1186/s12862-019-1394-3>.
- Feldman, D., Yarden, O., Hadar, Y., 2020. Seeking the roles for fungal small-secreted proteins in affecting saprophytic lifestyles. *Front. Microbiol.* 11. <https://doi.org/10.3389/fmicb.2020.00455>.
- Feng, L., Wang, W., Cheng, J., Ren, Y., Zhao, G., Gao, C., Tang, Y., Liu, X., Han, W., Peng, X., Liu, R., Wang, L., 2007. Genome and proteome of long-chain alkane degrading *Geobacillus thermodenitrificans* NG80-2 isolated from a deep-subsurface oil reservoir. *Proc. Natl. Acad. Sci.* 104 (13), 5602–5607. <https://doi.org/10.1073/pnas.0609650104>.
- Ferroni, F.M., Smit, M.S., Opperman, D.J., 2014. Functional divergence between closely related Baeyer-Villiger monooxygenases from *Aspergillus flavus*. *J. Mol. Catal. B Enzym.* 107, 47–54. <https://doi.org/10.1016/j.molcatb.2014.05.015>.
- Filella, M., Turner, A., Arp, H.P.H., 2021. Editorial: plastics in the environment: understanding impacts and identifying solutions. *Front. Environ. Sci.* 9. <https://doi.org/10.3389/fenvs.2021.699971>.
- Frankenfeld, A.M., Ni, J., Ahmed, M., Hao, L., 2022. Protein contaminants matter: building universal protein contaminant libraries for DDA and DIA proteomics. *J. Proteome Res.* 21 (9), 2104–2113. <https://doi.org/10.1021/acs.jproteome.2c00145>.
- Gabriel, L., Brúna, T., Hoff, K.J., Ebel, M., Lomsadze, A., Borodovsky, M., Stanke, M., 2024. BRAKER3: fully automated genome annotation using RNA-seq and protein evidence with GeneMark-ETP, AUGUSTUS, and TSEBRA. *Genome Res.* 34 (5), 769–777. <https://doi.org/10.1101/gr.278090.123>.
- Gabriel, L., Hoff, K.J., Brúna, T., Borodovsky, M., Stanke, M., 2021. TSEBRA: transcript selector for BRAKER. *BMC Bioinf.* 22 (1), 566. <https://doi.org/10.1186/s12859-021-04482-0>.
- Gao, R., Liu, R., Sun, C., 2022. A marine fungus *Alternaria alternata* FB1 efficiently degrades polyethylene. *J. Hazard Mater.* 431, 128617. <https://doi.org/10.1016/j.jhazmat.2022.128617>.
- Geisler, D.J., Kong, A.T., Avtonomov, D.M., Yu, F., Leprevost, F. da V., Nesvizhskii, A.I., 2021. PTM-Shepherd: analysis and summarization of post-translational and chemical modifications from open search results. *Mol. Cell. Proteomics* 20, 100018. <https://doi.org/10.1074/mcp.TIR120.002216>.
- Giorgi, F.M., Bolger, A.M., Lohse, M., Usadel, B., 2010. Algorithm-driven artifacts in median polish summarization of microarray data. *BMC Bioinf.* 11 (1), 553. <https://doi.org/10.1186/1471-2105-11-553>.
- Gislason, M.H., Nielsen, H., Almagro Armenteros, J.J., Johansen, A.R., 2021. Prediction of GPI-anchored proteins with pointer neural networks. *Curr. Res. Biotechnol.* 3, 6–13. <https://doi.org/10.1016/j.crbiot.2021.01.001>.
- Gravouil, K., Ferru-Clément, R., Colas, S., Helye, R., Kadri, L., Bourdeau, L., Moumen, B., Mercier, A., Ferreira, T., 2017. Transcriptomics and lipidomics of the environmental strain *Rhodococcus ruber* point out consumption pathways and potential metabolic bottlenecks for polyethylene degradation. *Environ. Sci. Technol.* 51 (9), 5172–5181. <https://doi.org/10.1021/acs.est.7b00846>.
- Gregson, B.H., Metodiev, G., Metodiev, M.V., Golyshe, P.N., McKew, B.A., 2018. Differential protein expression during growth on medium versus long-chain alkanes in the obligate marine hydrocarbon-degrading bacterium *Thalassolituus oleivorans* MIL-1. *Front. Microbiol.* 9. <https://doi.org/10.3389/fmicb.2018.03130>.
- Grigoriev, I.V., Nikitin, R., Haridas, S., Kuo, A., Ohm, R., Otilar, R., Riley, R., Salamov, A., Zhao, X., Korzeniewski, F., Smirnova, T., Nordberg, H., Dubchak, I., Shabalov, I., 2014. MycoCosm portal: gearing up for 1000 fungal genomes. *Nucleic Acids Res.* 42 (D1), D699–D704. <https://doi.org/10.1093/nar/gkt1183>.
- Griss, J., Perez-Riverol, Y., Lewis, S., Tabb, D.L., Dianas, J.A., del-Toro, N., Rurik, M., Walzer, M., Kohlbacher, O., Hermjakob, H., Wang, R., Vizcaino, J.A., 2016. Recognizing millions of consistently unidentified spectra across hundreds of shotgun proteomics datasets. *Nat. Methods* 13 (8), 651–656. <https://doi.org/10.1038/nmeth.3902>.
- Grüning, B., Dale, R., Sjödin, A., Chapman, B.A., Rowe, J., Tomkins-Tinch, C.H., Valieris, R., Köster, J., Team, T.B., 2018. Bioconda: sustainable and comprehensive software distribution for the life sciences. *Nat. Methods* 15 (7), 475–476. <https://doi.org/10.1038/s41592-018-0046-7>.
- Gulmine, J.V., Janissek, P.R., Heise, H.M., Akcelrud, L., 2002. Polyethylene characterization by FTIR. *Polym. Test.* 21 (5), 557–563. [https://doi.org/10.1016/S0142-9418\(01\)00124-6](https://doi.org/10.1016/S0142-9418(01)00124-6).
- Haas, B.J., Papanicolaou, A., Yassour, M., Grabherr, M., Blood, P.D., Bowden, J., Couger, M.B., Eccles, D., Li, B., Lieber, M., MacManes, M.D., Ott, M., Orvis, J., Pochet, N., Strozzi, F., Weeks, N., Westerman, R., Williams, T., Dewey, C.N., Henschel, R., Regev, A., 2013. De novo transcript sequence reconstruction from RNA-seq using the Trinity platform for reference generation and analysis. *Nature Protoc.* 8 (8), 1494–1512. <https://doi.org/10.1038/nprot.2013.084>.
- Haas, B.J., Zeng, Q., Pearson, M.D., Cuomo, C.A., Wortman, J.R., 2011. Approaches to fungal genome annotation. *Mycology* 2 (3), 118–141. <https://doi.org/10.1080/21501203.2011.606851>.
- Hakkarainen, M., Albertsson, A.-C., 2004. Environmental degradation of polyethylene. In: Albertsson, A.-C. (Ed.), *Long Term Properties of Polyolefins*. Springer Berlin Heidelberg, pp. 177–200. <https://doi.org/10.1007/b13523>.
- Ho, B., Baryshnikova, A., Brown, G.W., 2018. Unification of protein abundance datasets yields a quantitative *Saccharomyces cerevisiae* proteome. *Cell Sys.* 6 (2), 192–205.e3. <https://doi.org/10.1016/j.cels.2017.12.004>.
- Hoang, D.T., Chernomor, O., von Haeseler, A., Minh, B.Q., Vinh, L.S., 2018. UFBoot2: improving the ultrafast bootstrap approximation. *Mol. Biol. Evol.* 35 (2), 518–522. <https://doi.org/10.1093/molbev/msx281>.
- Holt, C., Yandell, M., 2011. MAKER2: an annotation pipeline and genome-database management tool for second-generation genome projects. *BMC Bioinf.* 12 (1). <https://doi.org/10.1186/1471-2105-12-491>.
- Jin, J., Arciszewski, J., Auclair, K., Jia, Z., 2023. Enzymatic polyethylene biorecycling: confronting challenges and shaping the future. *J. Hazard Mater.* 460, 132449. <https://doi.org/10.1016/j.jhazmat.2023.132449>.
- Katoh, K., Standley, D.M., 2013. MAFFT multiple sequence alignment software version 7: improvements in performance and usability. *Mol. Biol. Evol.* 30 (4), 772–780. <https://doi.org/10.1093/molbev/mst010>.
- Kim, S., Pevzner, P.A., 2014. MS-GF+ makes progress towards a universal database search tool for proteomics. *Nat. Commun.* 5 (1), 5277. <https://doi.org/10.1038/ncomms6277>.
- Kjærboelling, I., Vesth, T., Frisvad, J.C., Nybo, J.L., Theobald, S., Kildgaard, S., Petersen, T.I., Kuo, A., Sato, A., Lyhne, E.K., Kogle, M.E., Wiebenga, A., Kun, R.S., Lubbers, R.J.M., Mäkelä, M.R., Barry, K., Chovatia, M., Clum, A., Daum, C., Andersen, M.R., 2020. A comparative genomics study of 23 *Aspergillus* species from section Flavi. *Nat. Commun.* 11 (1). <https://doi.org/10.1038/s41467-019-14051-y>.
- Klopfenstein, D.V., Zhang, L., Pedersen, B.S., Ramirez, F., Vesztrocy, A.W., Naldi, A., Mungall, C.J., Yunes, J.M., Botvinnik, O., Weigel, M., Dampier, W., Dessimoz, C., Flick, P., Tang, H., 2018. GOATOOLS: a python library for gene ontology analyses. *Sci. Rep.* 8 (1), 1–17. <https://doi.org/10.1038/s41598-018-28948-z>.
- Kong, A.T., Leprevost, F.V., Avtonomov, D.M., Mellacheruvu, D., Nesvizhskii, A.I., 2017. MSFragger: ultrafast and comprehensive peptide identification in mass spectrometry-based proteomics. *Nat. Methods* 14 (5), 513–520. <https://doi.org/10.1038/nmeth.4256>.
- Kovács, R.L., Csontos, M., Gyöngyösi, S., Elek, J., Parditka, B., Deák, G., Kuki, Á., Kéki, S., Erdélyi, Z., 2021. Surface characterization of plasma-modified low density polyethylene by attenuated total reflectance fourier-transform infrared (ATR-FTIR) spectroscopy combined with chemometrics. *Polym. Test.* 96, 107080. <https://doi.org/10.1016/j.polymertesting.2021.107080>.
- Kuznetsov, D., Teigenfeldt, F., Manni, M., Seppey, M., Berkeley, M., Kriventseva, E.V., Zdobnov, E.M., 2023. OrthoDB v11: annotation of orthologs in the widest sampling of organismal diversity. *Nucleic Acids Res.* 51 (D1), D445–D451. <https://doi.org/10.1093/nar/gkac998>.
- Lazear, M.R., 2023. Sage: an open-source tool for fast proteomics searching and quantification at scale. *J. Proteome Res.* 22 (11), 3652–3659. <https://doi.org/10.1021/acs.jproteome.3c00486>.
- Levasseur, A., Drula, E., Lombard, V., Coutinho, P.M., Henrissat, B., 2013. Expansion of the enzymatic repertoire of the CAZy database to integrate auxiliary redox enzymes. *Biotechnol. Biofuels* 6 (1), 1–14. <https://doi.org/10.1186/1754-6834-6-41>.
- Li, J., Xu, Y., Song, Q., Zhang, S., Xie, L., Yang, J., 2021. Transmembrane transport mechanism of n-hexadecane by *Candida tropicalis*: kinetic study and proteomic analysis. *Ecotoxicol. Environ. Saf.* 209, 111789. <https://doi.org/10.1016/j.ecoenv.2020.111789>.
- Liao, S., Tung, E.T.K., Zheng, W., Chong, K., Xu, Y., Dai, P., Guo, Y., Bartlam, M., Yuen, K.-Y., Rao, Z., 2010. Crystal structure of the Mp1p ligand binding domain 2 reveals its function as a fatty acid-binding protein. *J. Biol. Chem.* 285 (12), 9211–9220. <https://doi.org/10.1074/jbc.M109.057760>.
- Liu, J., Chen, S., Zhao, B., Li, G., Ma, T., 2022. A novel FadL homolog, AltL, mediates transport of long-chain alkanes and fatty acids in *Acinetobacter venetianus* RAG-1. *Appl. Environ. Microbiol.* 88 (20), e01294. <https://doi.org/10.1128/aem.01294-22.22>.
- Maia, M., Nunes, F.M., 2013. Authentication of beeswax (*Apis mellifera*) by high-temperature gas chromatography and chemometric analysis. *Food Chem.* 136 (2), 961–968. <https://doi.org/10.1016/j.foodchem.2012.09.003>.
- Manni, M., Berkeley, M.R., Seppey, M., Simão, F.A., Zdobnov, E.M., 2021. BUSCO update: novel and streamlined workflows along with broader and deeper

- phylogenetic coverage for scoring of eukaryotic, prokaryotic, and viral genomes. *Mol. Biol. Evol.* 38 (10), 4647–4654. <https://doi.org/10.1093/molbev/msab199>.
- Maseme, M.J., Pennec, A., van Marwijk, J., Opperman, D.J., Smit, M.S., 2020. CYP50E3: a novel self-sufficient  $\omega$ -7 In-Chain hydroxylase. *Angew. Chem. Int. Ed.* 59 (26), 10359–10362. <https://doi.org/10.1002/anie.202001055>.
- May, D.H., Tamura, K., Noble, W.S., 2017. Param-medic: a tool for improving MS/MS database search yield by optimizing parameter settings. *J. Proteome Res.* 16 (4), 1817–1824. <https://doi.org/10.1021/acs.jproteome.7b00028>.
- Minh, B.Q., Hahn, M.W., Lanfear, R., 2020a. New methods to calculate concordance factors for phylogenomic datasets. *Mol. Biol. Evol.* 37 (9), 2727–2733. <https://doi.org/10.1093/molbev/msaa106>.
- Minh, B.Q., Schmidt, H.A., Chernomor, O., Schrempf, D., Woodhams, M.D., von Haeseler, A., Lanfear, R., 2020b. IQ-TREE 2: new models and efficient methods for phylogenetic inference in the genomic era. *Mol. Biol. Evol.* 37 (5), 1530–1534. <https://doi.org/10.1093/molbev/msaa015>.
- Montazer, Z., Habibi Najafi, M.B., Levin, D.B., 2020. Challenges with verifying microbial degradation of polyethylene. *Polymers* 12 (1). <https://doi.org/10.3390/polym12010123>.
- Nakamiya, K., Sakasita, G., Ooi, T., Kinoshita, S., 1997. Enzymatic degradation of polystyrene by hydroquinone peroxidase of *Azotobacter beijerinckii* HM121. *J. Ferment. Bioeng.* 84, 480–482. <https://api.semanticscholar.org/CorpusID:83693430>.
- Napolitano, R., Juárez, M.P., 1997. Entomopathogenic fungi degrade epicuticular hydrocarbons of *Triatoma infestans*. *Arch. Biochem. Biophys.* 344 (1), 208–214. <https://doi.org/10.1006/abbi.1997.0163>.
- Olmedo, A., Aranda, C., del Río, J.C., Kiebišt, J., Scheibner, K., Martínez, A.T., Gutiérrez, A., 2016. From alkanes to carboxylic acids: terminal oxygenation by a fungal peroxidase. *Angew. Chem. Int. Ed.* 55 (40), 12248–12251. <https://doi.org/10.1002/anie.201605430>.
- Pantelic, B., Siaperas, R., Budin, C., de Boer, T., Topakas, E., Nikodinovic-Runic, J., 2024. Proteomic examination of polyester-polyurethane degradation by *Streptomyces* sp. PU10: diverting polyurethane intermediates to secondary metabolite production. *Microb. Biotechnol.* 17 (3), e14445. <https://doi.org/10.1111/1751-7915.14445>.
- Patel, H., Ewels, P., Manning, J., Garcia, M.U., Peltzer, A., Hammarén, R., Botvinnik, O., Talbot, A., Sturm, G., Zepper, M., Moreno, D., Vemuri, P., Binzer-Panchal, M., Greenberg, E., silviamorins, Pantano, L., Syme, R., Kelly, G., Gabernet, G., bot, nf-core, 2024. *nf-core/rnaseq: nf-core/rnaseq v3.17.0 - neon newt*. Zenodo. <https://doi.org/10.5281/zenodo.13986791>.
- Paysan-Lafosse, T., Blum, M., Chuguransky, S., Grego, T., Pinto, B.L., Salazar, G.A., Bileschi, M.L., Bork, P., Bridge, A., Colwell, L., Gough, J., Haft, D.H., Letunic, I., Marchler-Bauer, A., Mi, H., Natale, D.A., Orengo, C.A., Pandurangan, A.P., Rivoire, C., et al., 2023. InterPro in 2022. *Nucleic Acids Res.* 51 (D1), D418–D427. <https://doi.org/10.1093/nar/gkac993>.
- Perera, M., Wijesundera, S., Wijayarathna, C.D., Seneviratne, G., Jayasena, S., 2022. Identification of long-chain alkane-degrading (LadA) monooxygenases in *Aspergillus flavus* via in silico analysis. *Front. Microbiol.* 13. <https://doi.org/10.3389/fmicb.2022.898456>.
- Perez-Riverol, Y., Bai, J., Bandla, C., García-Seisdedos, D., Hewapathirana, S., Kamatchinathan, S., Kundu, D.J., Prakash, A., Frericks-Zipper, A., Eisenacher, M., Walzer, M., Wang, S., Brazma, A., Vizcaíno, J.A., 2022. The PRIDE database resources in 2022: a hub for mass spectrometry-based proteomics evidences. *Nucleic Acids Res.* 50 (D1), D543–D552. <https://doi.org/10.1093/nar/gkab1038>.
- Peter, S., Kinne, M., Wang, X., Ullrich, R., Kayser, G., Groves, J.T., Hofrichter, M., 2011. Selective hydroxylation of alkanes by an extracellular fungal peroxidase. *FEBS J.* 278 (19), 3667–3675. <https://doi.org/10.1111/j.1742-4658.2011.08285.x>.
- Pivato, A.F., Miranda, G.M., Prichula, J., Lima, J.E.A., Ligabue, R.A., Seixas, A., Trentin, D.S., 2022. Hydrocarbon-based plastics: progress and perspectives on consumption and biodegradation by insect larvae. *Chemosphere* 293, 133600. <https://doi.org/10.1016/j.chemosphere.2022.133600>.
- Plastics Europe, 2024. The circular economy for plastics. A European analysis 2024. <http://plasticseurope.org/knowledge-hub/the-circular-economy-for-plastics-a-european-analysis-2024/>.
- Prijbelski, A., Antipov, D., Meleshko, D., Lapidus, A., Korobeynikov, A., 2020. Using SPAdes De Novo Assembler. *Curr. Protoc. Bioinf.* 70 (1), 1–29. <https://doi.org/10.1002/cpbi.102>.
- Puspitasari, N., Tsai, S.-L., Lee, C.-K., 2021. Fungal Hydrophobin RoIA enhanced PETase hydrolysis of polyethylene terephthalate. *Appl. Biochem. Biotechnol.* 193 (5), 1284–1295. <https://doi.org/10.1007/s12010-020-03358-y>.
- Renwei, G., Mingyue, D., Siqi, J., Zheng, Z., Komal, C., Qirong, S., Feng, C., S, D.L., 2020. The evolutionary and functional paradox of cerato-platanins in fungi. *Appl. Environ. Microbiol.* 86 (13), e00696. <https://doi.org/10.1128/AEM.00696-20>.
- Restrepo-Florez, J.M., Bassi, A., Thompson, M.R., 2014. Microbial degradation and deterioration of polyethylene - a review. *Int. Biodeterior. Biodegrad.* 88, 83–90. <https://doi.org/10.1016/j.ibiod.2013.12.014>.
- Robinson, M.D., McCarthy, D.J., Smyth, G.K., 2010. edgeR: a bioconductor package for differential expression analysis of digital gene expression data. *Bioinformatics* 26 (1), 139–140. <https://doi.org/10.1093/bioinformatics/btp616>.
- Rojo, F., 2009. Degradation of alkanes by bacteria. *Environ. Microbiol.* 11 (10), 2477–2490. <https://doi.org/10.1111/j.1462-2920.2009.01948.x>.
- Saier Jr, M.H., Reddy, V.S., Moreno-Hagelsieb, G., Hendargo, K.J., Zhang, Y., Iddamsetty, V., Lam, K.J.K., Tian, N., Russum, S., Wang, J., Medrano-Soto, A., 2021. The Transporter Classification Database (TCDB): 2021 update. *Nucleic Acids Res.* 49 (D1), D461–D467. <https://doi.org/10.1093/nar/gkaa1004>.
- Sathiyabama, M., Boomija, R.V., Sathiyamoorthy, T., Mathivanan, N., Balaji, R., 2024. Mycodegradation of low-density polyethylene by *Cladosporium sphaerospermum*, isolated from platisphere. *Sci. Rep.* 14 (1), 8351. <https://doi.org/10.1038/s41598-024-59032-4>.
- Schurch, N.J., Schofield, P., Gierliński, M., Cole, C., Sherstnev, A., Singh, V., Wrobel, N., Gharbi, K., Simpson, G.G., Owen-Hughes, T., Blaxter, M., Barton, G.J., 2016. How many biological replicates are needed in an RNA-seq experiment and which differential expression tool should you use? *RNA* 22 (6), 839–851. <https://doi.org/10.1261/rna.053959.115>.
- Shinsaku, O., Hiroshi, M., Toru, T., Youhei, Y., Fumihiko, H., Katsuya, G., Tasuku, N., Keitsu, A., 2006. Novel hydrophobic surface binding protein, HsbA, produced by *Aspergillus oryzae*. *Appl. Environ. Microbiol.* 72 (4), 2407–2413. <https://doi.org/10.1128/AEM.72.4.2407-2413.2006>.
- Spina, F., Tummino, M.L., Poli, A., Prigione, V., Ilieva, V., Cocconcelli, P., Puglisi, E., Bracco, P., Zanetti, M., Varese, G.C., 2021. Low density polyethylene degradation by filamentous fungi. *Environ. Pollut.* 274, 116548. <https://doi.org/10.1016/j.envpol.2021.116548>.
- Steenwyk, J.L., Balamurugan, C., Raja, H.A., Gonçalves, C., Li, N., Martin, F., Berman, J., Oberlies, N.H., Gibbons, J.G., Goldman, G.H., Geiser, D.M., Houbraeken, J., Rokas, A., 2024. Phylogenomics reveals extensive misidentification of fungal strains from the genus *Aspergillus*. *Microbiol. Spectr.* 12 (4), e03980. <https://doi.org/10.1128/spectrum.03980-23>.
- Steenwyk, J.L., Rokas, A., 2021. Orthofisher: a broadly applicable tool for automated gene identification and retrieval. *G3 Genes/Genomes/Genetics* 11 (9), jkab250. <https://doi.org/10.1093/g3journal/jkab250>.
- Tao, X., Ouyang, H., Zhou, A., Wang, D., Matlock, H., Morgan, J.S., Ren, A.T., Mu, D., Pan, C., Zhu, X., Han, A., Zhou, J., 2023. Polyethylene degradation by a *Rhodococcus* strain isolated from naturally weathered plastic waste enrichment. *Environ. Sci. Technol.* 57 (37), 13901–13911. <https://doi.org/10.1021/acs.est.3c03778>.
- Tarailo-Graovac, M., Chen, N., 2009. Using RepeatMasker to identify repetitive elements in genomic sequences. *Curr. Protoc. Bioinf.* (4.10.1–4.10.14). <https://doi.org/10.1002/0471250953.bi0410s25.chapter4>.
- Taxeidis, G., Nikolaivits, E., Nikodinovic-Runic, J., Topakas, E., 2024. Mimicking the enzymatic plant cell wall hydrolysis mechanism for the degradation of polyethylene terephthalate. *Environ. Pollut.* 356, 124347. <https://doi.org/10.1016/j.envpol.2024.124347>.
- Taxeidis, G., Nikolaivits, E., Siaperas, R., Gkoutela, C., Vouyiouka, S., Pantelic, B., Nikodinovic-Runic, J., Topakas, E., 2023. Triggering and identifying the polyurethane and polyethylene-degrading machinery of filamentous fungi secretomes. *Environ. Pollut.* 325, 121460. <https://doi.org/10.1016/j.envpol.2023.121460>.
- Ter-Hovhannisyan, V., Lomsadze, A., Chernoff, Y.O., Borodovsky, M., 2008. Gene prediction in novel fungal genomes using an ab initio algorithm with unsupervised training. *Genome Res.* 18 (12), 1979–1990. <https://doi.org/10.1101/gr.081612.108>.
- Teufel, F., Almagro Armenteros, J.J., Johansen, A.R., Gíslason, M.H., Pihl, S.I., Tsirigos, K.D., Winther, O., Brunak, S., von Heijne, G., Nielsen, H., 2022. SignalP 6.0 predicts all five types of signal peptides using protein language models. *Nat. Biotechnol.* <https://doi.org/10.1038/s41587-021-01156-3>.
- Thevenieau, P., Le Dall, M.-T., Nthangeni, B., Mauersberger, S., Marchal, R., Nicaud, J.-M., 2007. Characterization of *Yarrowia lipolytica* mutants affected in hydrophobic substrate utilization. *Fungal Genet. Biol.* 44 (6), 531–542. <https://doi.org/10.1016/j.fgb.2006.09.001>.
- Thompson, R.C., Swan, S.H., Moore, C.J., vom Saal, F.S., 2009. Our plastic age. *Phil. Trans. Biol. Sci.* 364 (1526), 1973–1976. <https://doi.org/10.1098/rstb.2009.0054>.
- Thumulari, V., Almagro Armenteros, J.J., Johansen, A.R., Nielsen, H., Winther, O., 2022. DeepLoc 2.0: multi-label subcellular localization prediction using protein language models. *Nucleic Acids Res.* 50 (W1), W228–W234. <https://doi.org/10.1093/nar/gkac278>.
- Velez, P., Gasca-Pineda, J., Riquelme, M., 2020. Cultivable fungi from deep-sea oil reserves in the Gulf of Mexico: genetic signatures in response to hydrocarbons. *Mar. Environ. Res.* 153, 104816. <https://doi.org/10.1016/j.marenvres.2019.104816>.
- Viguera, G., Shirai, K., Hernández-Guerrero, M., Morales, M., Revah, S., 2014. Growth of the fungus *Paecilomyces lilacinus* with n-hexadecane in submerged and solid-state cultures and recovery of hydrophobin proteins. *Process Biochem.* 49 (10), 1606–1611. <https://doi.org/10.1016/j.procbio.2014.06.015>.
- Wang, W., Shao, Z., 2014. The long-chain alkane metabolism network of *Alcanivorax dieselolei*. *Nat. Commun.* 5 (1), 5755. <https://doi.org/10.1038/ncomms6755>.
- Wang, Y., Zhao, X., Wang, J., Weng, Y., Wang, Y., Li, X., Han, X., 2023. Ingestion preference and efficiencies of different polymerization types foam plastics by *Tenebrio molitor* larvae, associated with changes of both core gut bacterial and fungal microbiomes. *J. Environ. Chem. Eng.* 11 (5), 110801. <https://doi.org/10.1016/j.jece.2023.110801>.
- Wolski, W.E., Nanni, P., Grossmann, J., d'Errico, M., Schlapbach, R., Panse, C., 2023. Proflqua: a comprehensive R-Package for proteomics differential expression analysis. *J. Proteome Res.* 22 (4), 1092–1104. <https://doi.org/10.1021/acs.jproteome.2c00441>.
- Wood, D.E., Lu, J., Langmead, B., 2019. Improved metagenomic analysis with Kraken 2. *Genome Biol.* 20 (1), 1–13. <https://doi.org/10.1186/s13059-019-1891-0>.
- Wróbel, M., Szymańska, S., Kowalkowski, T., Hryniewicz, K., 2023. Selection of microorganisms capable of polyethylene (PE) and polypropylene (PP) degradation. *Microbiol. Res.* 267, 127251. <https://doi.org/10.1016/j.micres.2022.127251>.
- Yamada-Onodera, K., Mukumoto, H., Katsuyaya, Y., Saiganji, A., Tani, Y., 2001. Degradation of polyethylene by a fungus, *Penicillium simplicissimum* YK. *Polym. Degrad. Stabil.* 72 (2), 323–327. [https://doi.org/10.1016/S0141-3910\(01\)00027-1](https://doi.org/10.1016/S0141-3910(01)00027-1).
- Zadjelovic, V., Erni-Cassola, G., Obrador-Viel, T., Lester, D., Eley, Y., Gibson, M.I., Dorador, C., Golyshin, P.N., Black, S., Wellington, E.M.H., Christie-Oleza, J.A., 2022.

- A mechanistic understanding of polyethylene biodegradation by the marine bacterium *Alcanivorax*. *J. Hazard Mater.* 436. <https://doi.org/10.1016/j.jhazmat.2022.129278>.
- Zafeiropoulos, H., Gioti, A., Ninidakis, S., Potirakis, A., Paragkamian, S., Angelova, N., Antoniou, A., Danis, T., Kaitetzidou, E., Kasapidis, P., Kristoffersen, J.B., Papadogiannis, V., Pavlouti, C., Ha, Q.V., Lagnel, J., Pattakos, N., Perantinos, G., Sidirokastritis, D., Vavilis, P., et al., 2021. Os and Is in marine molecular research: a regional HPC perspective. *GigaScience* 10 (8), giab053. <https://doi.org/10.1093/gigascience/giab053>.
- Zampolli, J., Mangiagalli, M., Vezzini, D., Lasagni, M., Ami, D., Natalello, A., Arrigoni, F., Bertini, L., Lotti, M., Di Gennaro, P., 2023. Oxidative degradation of polyethylene by two novel laccase-like multicopper oxidases from *Rhodococcus opacus* R7. *Environ. Technol. Innovat.* 32. <https://doi.org/10.1016/j.eti.2023.103273>.
- Zampolli, J., Orro, A., Manconi, A., Ami, D., Natalello, A., Di Gennaro, P., 2021. Transcriptomic analysis of *Rhodococcus opacus* R7 grown on polyethylene by RNA-seq. *Sci. Rep.* 11 (1). <https://doi.org/10.1038/s41598-021-00525-x>.
- Zerva, A., Pentari, C., Ferousi, C., Nikolavits, E., Karnaouri, A., Topakas, E., 2021. Recent advances on key enzymatic activities for the utilisation of lignocellulosic biomass. *Bioresour. Technol.* 342, 126058. <https://doi.org/10.1016/j.biortech.2021.126058>.
- Zhang, J., Gao, D., Li, Q., Zhao, Y., Li, L., Lin, H., Bi, Q., Zhao, Y., 2020a. Biodegradation of polyethylene microplastic particles by the fungus *Aspergillus flavus* from the guts of wax moth *Galleria mellonella*. *Sci. Total Environ.* 704, 135931. <https://doi.org/10.1016/j.scitotenv.2019.135931>.
- Zhang, J., Hao, H., Wu, X., Wang, Q., Chen, M., Feng, Z., Chen, H., 2020b. The functions of glutathione peroxidase in ROS homeostasis and fruiting body development in *Hypsizygus marmoreus*. *Appl. Microbiol. Biotechnol.* 104 (24), 10555–10570. <https://doi.org/10.1007/s00253-020-10981-6>.
- Zheng, J., Ge, Q., Yan, Y., Zhang, X., Huang, L., Yin, Y., 2023. dbCAN3: automated carbohydrate-active enzyme and substrate annotation. *Nucleic Acids Res.* 51 (W1), W115–W121. <https://doi.org/10.1093/nar/gkad328>.